Pergamon

0277-5387(95)00181-6

Polyhedron Vol. 14, No. 23-24, pp. 3537-3544, 1995

0277-5387/95 $9.50+0.00

STUDIES ON THE BAND STRUCTURES OF SOME LAVES-PHASE COMPOUNDS*

SHU-HUI CAI and CHUN-WAN LIU†

Fujian Institute of Research on the Structure of Matter, Chinese Academy of Sciences and State Key Laboratory of Structural Chemistry, Fuzhou, Fujian 350002, P.R.C

(*Received* 21 *December* 1994; *accepted* 12 *April* 1995)

Abstract—The band structures of several real and dummy Laves-phase compounds, AB_2 (A = Zr, Hf; B = Re, V, Mo), have been calculated by use of the tight-binding method within the extended Hückel approximation (EHT). The energy bands, the densities of states and the crystal orbital overlap populations of these compounds are discussed. A new relationship between the bonding property and the superconducting transition temperature (T_c) of these compounds is revealed.

The theoretical investigation of superconductivity has been an interesting field for many years. Chemists have been trying to find some relationship between the superconducting transition temperature (T_c) and chemical bonding in the superconducting compounds. Our previous work[1,2] has shown that in some superconducting A15 and Chevrel phase compounds, the relative values of T_c can be related to their metal–metal bonding strength. Our work has been extended to the study of another class of superconducting compounds, the Laves phases. The so-called "Laves-phase" compounds are the intermetallic compounds expressed as AB_2 (both A and B are metal atoms).[3] In general, the ratio of atomic radii r_A/r_B determines the types of crystal structures. Theoretically, it is calculated as $r_A/r_B = 1.225$, but it actually ranges from 1.1 to 1.6. Their crystal structures are classified into three types, i.e. the $MgCu_2$ (C15) structure (space group: *Fd3m*), the $MgZn_2$(C14) structure (space group: $P6_3/mmc$) and the $MgNi_2$(C36) structure (space group: $P6_3/mmc$). Most of the Laves phases belong to the structural type C15. Many of them exhibit a wide range of electrical, magnetic and alloying properties. Almost all of the superconducting Laves phases belong to two structural types, C15 and C14.

Although there are about 500 known Laves-phase compounds, little experimental or theoretical research work has been carried out on them. For superconducting compounds, much experimental work was concentrated on the study of ZrV_2, HfV_2 and their pseudo-binary compounds because of their high superconducting transition temperatures (T_c) and high upper critical field (H_{c_2}). On the other hand, the complexity of their crystal structures makes theoretical investigation difficult. The first calculation about the Laves phases was made by Koelling *et al.*[4a] who calculated the band structure of Zr in a diamond lattice within an augmented-plane-wave (APW) scheme to model a $ZrZn_2$ crystal and found good agreement with the existing data. Later calculations include the linearized muffin-tin orbital (LMTO) calculations for $ZrZn_2$ and ZrV_2 by Jarlborg and Freeman,[5] for $BaRh_2$ and $LaRh_2$ by Asokamani *et al.*,[6] for YRh_2 and $LaRh_2$ by Pauline *et al.*,[7] for ABi_2 (A = K, Rb, Cs) by Sankaralingam *et al.*,[8] for ZrV_2 by Lerch *et al.*[9] and for MV_2 (M = Zr, Hf, Ta) by Chu *et al.*,[10] the non-self-consistent relativistic APW treatment for $ZrZn_2$ by deGroot *et al.*,[11] a self-consistent APW approach for ZrV_2 by Klein *et al.*,[12] the all-electron full-potential linearized-augmented-plane-wave (FLAPW) calculations for $ZrZn_2$ and ZrV_2 by Huang *et al.*,[13]

*Project supported by the National Natural Science Foundation of China and the Foundation of the State Key Laboratory of Structural Chemistry of China.

†Author to whom correspondence should be addressed.

as well as the self-consistent Korringa–Kohn–Rostoker (KKR) calculations for $ZrMn_2$ and AFe_2 (A = Ti, Nb, Sc, Mo, Hf, Ta, W) by Ishida *et al.*[14] All above Laves-phase compounds calculated belong to the C15 structural type except $ZrMn_2$ and AFe_2. The common results deduced were that, except for $TiBe_2$ and $ZrZn_2$, their densities of states (DOSs) are all characterized by the DOSs of atom B around the Fermi level. Johnston and Hoffmann[15] also discussed their structure-electron count and deformation-electron count correlations based on extended Hückel band calculations on model AB_2 compounds with both cubic and hexagonal structures and on the B sub-net along. And there are some main group metal Laves phases studied by Nesper.[16] However, few theoretical investigations on superconducting Laves-phase compounds, to our knowledge, have been published from the viewpoint of chemical bondings. In this paper, we shall carry out tight-binding band calculations, in the extended Hückel approximation (EHT), of some superconducting Laves-phase compounds to shed light on the dependence of T_c on their electronic structures and chemical bonding.

CALCULATIONS

Hoffmann's NNEW3 program was used to calculate the energy bands, the densities of states [DOS or N(E)] and the crystal orbital overlap populations (COOP). The semi-empirical parameters for the extended Hückel calculations are listed in Table 1,[17–22] where H_{ii} represents the ionization energy of the ith orbital,[17] ξ_1, ξ_2 and c_1, c_2 the orbital exponents and combination coefficients of the double-zeta basis functions,[18–22] respectively.

Since few superconducting compounds with C36 structure have been found, we shall calculate the compounds with C15 and C14 structures only. The crystal structures of C15 and C14 are shown in Fig. 1. The C15 structural type is cubic, having eight formula units per cell with A atoms forming a diamond structure and B atoms forming four interstitial tetrahedra in the A lattice. The C14 structure is a hexagonal layered structure. There are four A atoms, two B(2a) atoms at the 2a sites with symmetry $\bar{3}m$ and six B(6h) atoms at the 6h sites with symmetry mm in the unit cell. The compounds calculated are AB_2 (A = Zr, Hf; B = Re, V, Mo). Their crystal structure data are taken from refs 23–26.

RESULTS AND DISCUSSION

For the C14 structural type, we calculated for ARe_2 (A = Zr, Hf) compounds the band structures and the respective DOS curves, together with Re-atom partial contributions which are given in Figs 2 and 3. There are many flat curves in their band structures which come from the 60 atomic d orbitals of the 12 atoms in the unit cell. Some anisotropy can be found in both compounds and the conduction along the six-fold axis is relatively weak. From the atomic states we can guess that the upper flat curves are d bands of the atom A and the lower ones d bands of Re. Comparing the two band structures, we notice that the upper flat curves are lower in the $ZrRe_2$ case. The character of these curves

Table 1. Atomic parameters used in the calculations

Atom	Orbital	H_{ii} (eV)	ξ_1	ξ_2	c_1	c_2
V	$4s$	−6.74	1.60			
	$4p$	−4.71	1.60			
	$3d$	−8.00	4.75	1.50	0.4560	0.7520
Mo	$5s$	−7.10	1.96			
	$5p$	−3.54	1.90			
	$4d$	−8.56	4.54	1.90	0.5899	0.5899
Zr	$5s$	−6.84	1.817			
	$5p$	−5.01	1.776			
	$4d$	−8.61	3.835	1.505	0.6210	0.5769
Hf	$6s$	−7.50	2.214			
	$6p$	−5.66	2.166			
	$5d$	−7.00	4.360	1.709	0.7145	0.5458
Re	$6s$	−7.90	2.398			
	$6p$	−5.53	2.372			
	$5d$	−9.60	5.343	2.277	0.6662	0.5910

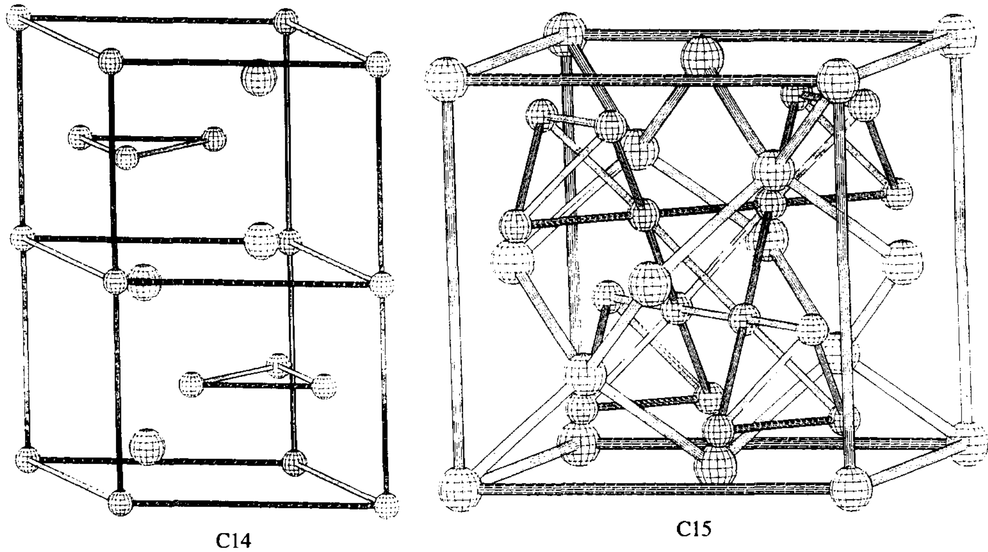

Fig. 1. The crystal structure of AB_2 compounds (large sphere: A atom, small sphere: B atom).

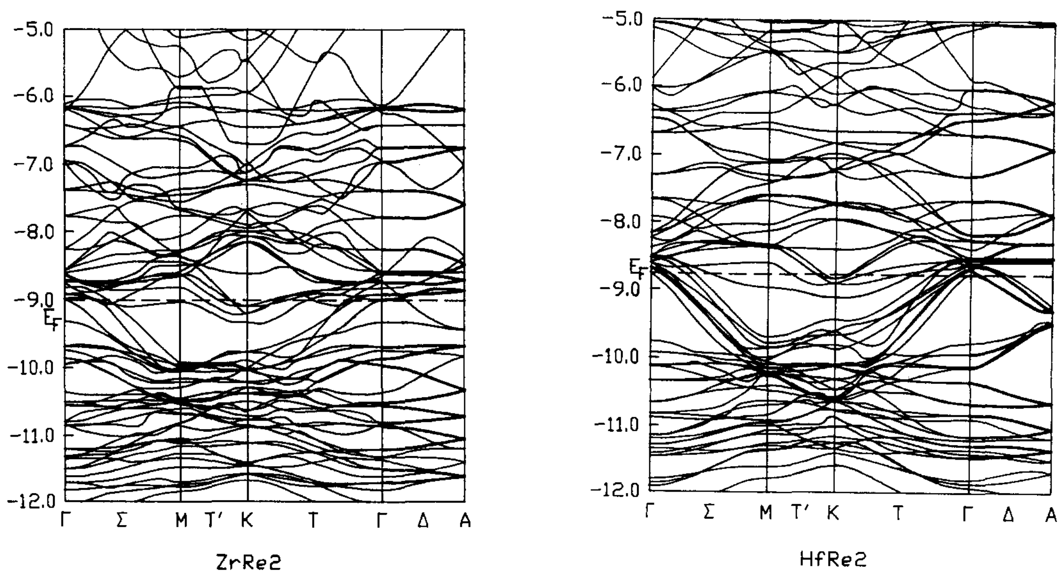

Fig. 2. Energy band structures of ARe_2 (A = Zr, Hf) near E_F. Heavy curves correspond to doubly degenerate bands.

becomes clearer with the DOS curves. The DOS curves of the C14 compounds have many sharp peaks which are due to flat curves. There are three sharp peaks of Re(6h) around the Fermi level and the peaks of Re(2a) in the same energy range. The Fermi level is situated at the valley of the DOS of Re(6h). Further atomic orbital projections will manifest their Re *d* character. The *d* states of A hybridize with those of Re in the wide range. The DOS of *d* states of Re(6h) is about three times as large as that of Re(2a) because of the different number of atoms in the unit cell. Their overall structures are very similar to each other in spite of their different circumstances, although there are some differences in the fine structures. The major peak of *d* bands of the atom A in the higher energy range shifts to the lower energy range when the atom changes from Hf to Zr. This shift is caused by the lowering of the potential of atom A. This implies that the hybridization between the *d* states of A and Re is stronger for $ZrRe_2$. In Fig. 3, the effect of the hybridization on the shape of the three peaks of Re(6h) is apparent.

Because the main contribution to the DOS at E_F comes from Re *d* states, which implies that the conducting electrons are mainly *d* electrons, we only discuss the Re—Re bonding in ARe_2. There are three types of Re—Re bonds:

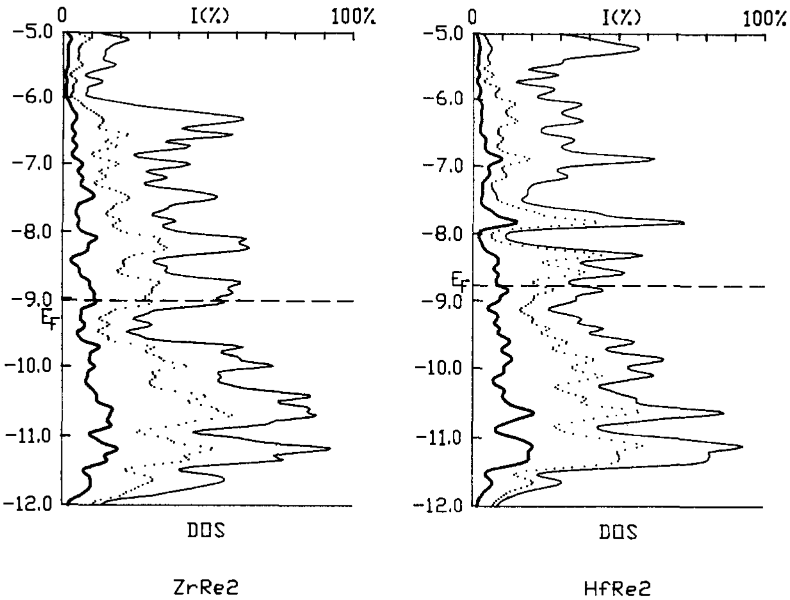

Fig. 3. Total and Re-projected densities of states for ARe_2 (A = Zr, Hf) near E_F [solid curve: total DOS, heavy curve: Re(2a)-projected, dotted curve: Re(6h)-projected].

Re(2a)—Re(6h)(Re_{ah}), Re(6h)—Re(6h) (uncapped triangle, Re^{u}_{hh}) and Re(6h)—Re(6h) (capped triangle, Re^{c}_{hh}) among which the bond length of Re^{u}_{hh} is the shortest. The crystal orbital overlap population (COOP) curves are plotted in Fig. 4. Clearly the Fermi level lies in the Re—Re antibonding area. The states at the Fermi level are predominantely related to the Re_{ah} bond. From Table 2 it is obvious that the order of bonding strength in each compound is as follows: $Re^{u}_{hh} > Re_{hh} > Re^{c}_{hh}$, and the COOP values of the Re_{ah} and Re^{c}_{hh} in both compounds are almost the same, respectively. This means that the difference in their conduction may be mainly influenced by

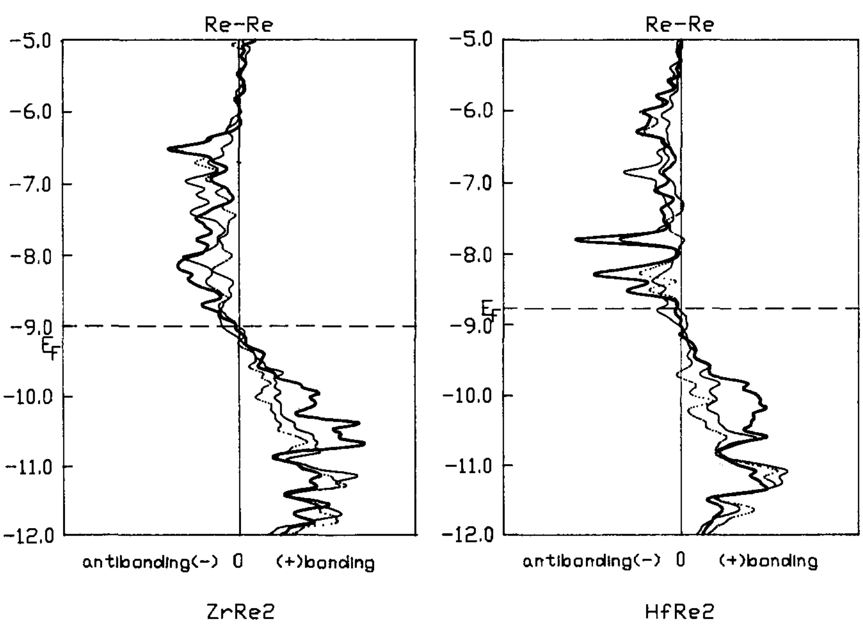

Fig. 4. Crystal orbital overlap populations (COOP) in ARe_2 (A = Zr, Hf) near E_F [solid curve: Re(2a)—Re(6h), dotted curve: Re(6h)—Re(6h) (capped), heavy curve: Re(6h)—Re(6h) (uncapped)].

Table 2. The experimental and calculated results for ARe_2

Compound	T_c (K)	$d^1_{B—B}$ (Å)	$P^1_{B—B}$	$d^2_{B—B}$ (Å)	$P^2_{B—B}$	$d^3_{B—B}$ (Å)	$P^3_{B—B}$
$ZrRe_2$	6.8	2.6312	0.400	2.6315	0.358	2.6305	0.458
$HfRe_2$	4.8	2.6255	0.408	2.6200	0.358	2.6190	0.491
$ZrRe_2^*$	/	2.6255	0.400	2.6200	0.362	2.6190	0.463
$HfRe_2^*$	/	2.6312	0.408	2.6315	0.355	2.6305	0.487

Note: $d^i_{B—B}$ indicates the distance between B atoms and $P^i_{B—B}$ the corresponding COOP value, the index $i = 1, 2, 3$ which denotes B(2a)—B(6h), B(6h)—B(6h) (capped) or B(6h)—B(6h) (uncapped), respectively. The compounds marked * are dummy ones constructed by interchanging the crystal structure data within the real pair.

the changes in the Re^u_{hh} bonding strength. This coincides with their anisotropy of conduction as discussed above.

Next we discuss the results of C15 compounds. Both AV_2 and AMo_2 (A = Zr, Hf) crystallize in cubic Laves phase C15 structural type. Their calculated results are shown in Figs 5–7 (only the results of AV_2 are demonstrated as examples). It can be found that their band structures are also complex and similar to each other. The increase in the number of valence electrons from V to Mo results in the rise of Fermi level. There exist some bands near E_F which are almost dispersionless in AV_2. From their DOS figures, it can be seen that the character of the bands near E_F is dominated by V or Mo d orbitals. The d states of A also have a rather important contribution in the energy range shown due to the hybridization with the other states. The fact that A states contribute more at the Fermi level in these phases compared with the ARe^2 phases is presumably because the potentials of the atom A and B become closer. For AV_2, the Fermi level is located near the maximum of a narrow peak in the DOS which arises from the almost dispersionless bands around the Fermi level, while in AMo_2, it is located very close to the valley. The value of the total DOS at E_F for AV_2 is large.

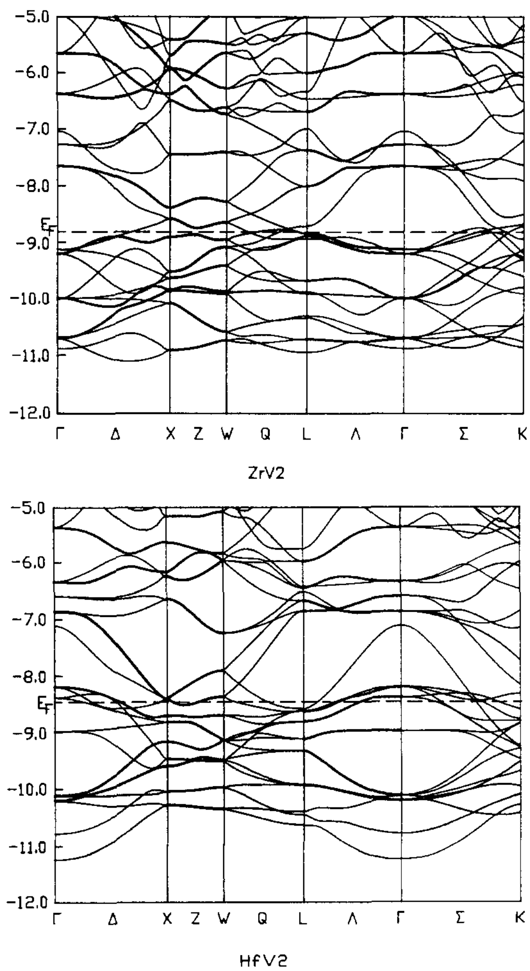

Fig. 5. Energy band structures of AV_2 (A = Zr, Hf) near E_F. Heavy curves correspond to doubly degenerate bands.

As to their bonding characters, let us consider their COOP analysis. There are three bonding types with short interatomic distances in the crystal: A—A bond, A—B bond and B—B bond. Because of the main contribution of the B atom at the Fermi level, only the COOP of A—B and B—B bonds are shown in Fig. 7. Obviously, the Fermi levels drop to the bonding range instead of being in the antibonding range as in ARe_2 cases due to the lower number of valence electrons for B = V and Mo. The bonding character is stronger for AV_2. The strength of the A—B bond is smaller than that of the B—B bond and the COOP values of A—B bonds are close. So we might conclude that the variation of their electronic mobility is largely determined by the strength of the B—B bond.

Tables 2 and 3 also reveal an interesting trend, that for all three choices of atom B the strength order of B—B bonds is exclusively Hf > Zr. In order to probe into this phenomenon, we further calculate some fictitious compounds corresponding to these three pairs by interchanging the atomic

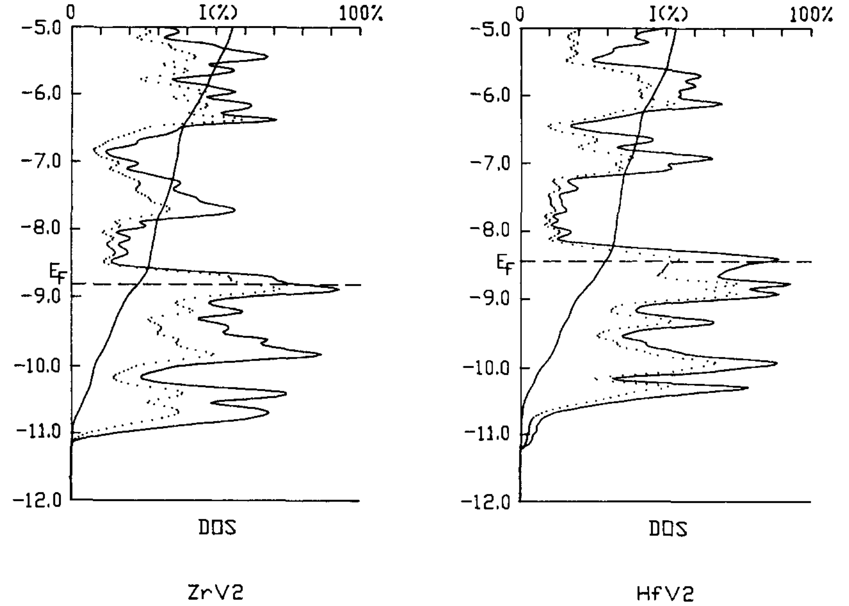

Fig. 6. Total, V-projected and integral densities of states for AV_2 (A = Zr, Hf) near E_F.

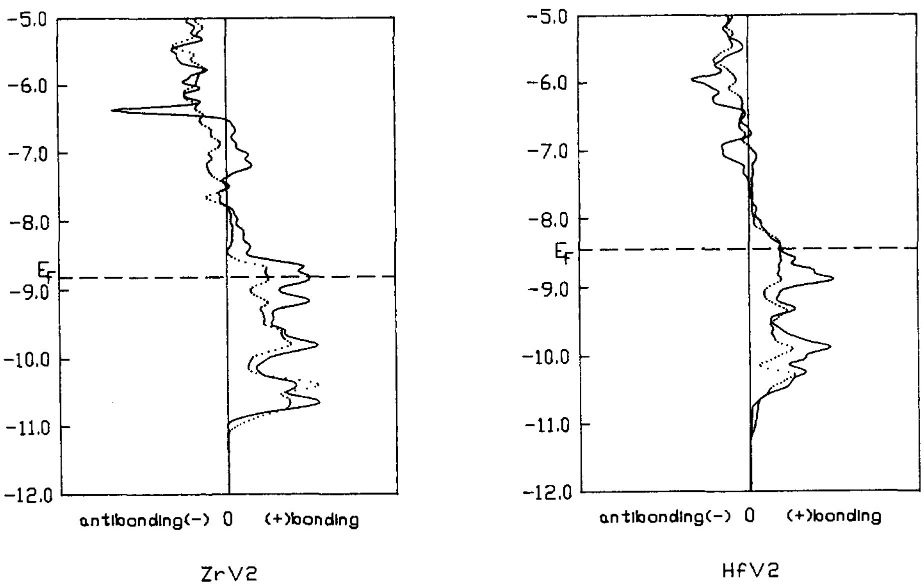

Fig. 7. Crystal orbital overlap populations (COOP) in AV_2 (A = Zr, Hf) near E_F (solid curve: V—V, dotted curve: A—V).

parameters of Zr and Hf within each pair only. The results are also listed in Tables 2 and 3 respectively. It is clear that the influence of distance on the COOP values can be ignored. The atom A mostly determines the changes in bonding strength. The corresponding values of each pair are almost the same as long as the same atomic parameters are used in calculations. This can also be seen from the calculations of the metals Zr and Hf (not shown here).

Now we consider the relationship between the electronic structures and the superconducting transition temperatures for these compounds. According to the Bardeen–Cooper–Schrieffer (BCS) equation,[27] the superconducting transition temperature (T_c) can be expressed as,

$$kT_c = 1.14\hbar\omega_D \exp\left(-\frac{1}{N(0)V}\right) \quad (1)$$

where ω_D is the lattice Debye frequency, $N(0)$ the electronic density of states at the Fermi energy, and V an effective potential including the attractive

Table 3. The experimental and calculated results for AV_2 and AMo_2

Compound	T_c(K)	d_{B-B}(Å)	P_{B-B}	d_{A-B}(Å)	P_{A-B}
ZrV_2	9.6	2.630	0.319	3.085	0.246
HfV_2	9.4	2.616	0.394	3.068	0.249
$ZrMo_2$	0.125	2.682	0.240	3.145	0.216
$HfMo_2$	0.07	2.671	0.269	3.132	0.211
ZrV_2^*	—	2.616	0.321	3.068	0.248
HfV_2^*	—	2.630	0.393	3.085	0.247
$ZrMo_2^*$	—	2.671	0.241	3.132	0.217
$HfMo_2^*$	—	2.682	0.268	3.145	0.209

Note: $d_{B-B}(d_{A-B})$ indicates the distance between B (A and B) atoms and P_{B-B} (P_{A-B}) the corresponding COOP value. The compounds marked * are dummy ones constructed by interchanging the crystal structure data within the real pairs.

electron–electron interaction mediated by phonons (V_{ph}) and the screened Coulomb repulsion V_o. McMillan[28] extended the BCS theory by introducing a term λ, i.e. the electron–phonon mass enhancement factor to describe the electron–phonon coupling strength [$\lambda \approx N(0)V$], which may be expressed as follows,

$$\lambda = \frac{N(0)\langle I^2 \rangle}{M\langle \omega^2 \rangle}. \qquad (2)$$

Here $\langle \omega^2 \rangle$ is the mean square phonon frequency, $\langle I^2 \rangle$ the electronic matrix element describing the electron–phonon interaction, and M the atomic mass. It contains two parts, the numerator representing the electronic part and the denominator the phonon part.

In view of the fact that λ is found inside the exponent, a small variation of λ will change the value of T_c more considerably than ω_D does. Thus we can focus our attention on the role of λ.

By virtue of eq. (2), it is obvious that the lower the $\langle \omega^2 \rangle$ the higher the T_c. As we know that $\langle \omega^2 \rangle$ is related to the lattice vibration, it has been pointed out[29,30] that the formation of strong covalent bonds, to a certain extent, competes with the superconductivity. A weakening of bonds may lead to a softening of average phonon spectrum and thus to the increase of T_c, i.e. the stronger the bonding, the lower the superconducting transition temperature. This has been demonstrated by our early work.[1,2] We have proved that for all the compounds under study the conduction electrons are of predominantly B d character and their mobility principally determined by the strength of B—B bonding. From Tables 2 and 3 we can see that the variation of experimentally measured T_c of the three series calculated can be explained based on the above concept. As we have shown above, the bonding strengths calculated in these three series are almost unrelated to their bond lengths. This implies that in these three series, the changes of T_c are largely related to the electronic effects of atom A rather than the steric effects, and Zr is preferred at higher T_c.

CONCLUSION

From the calculated band structures of several real and dummy Laves-phase compounds AB_2 (A = Zr, Hf; B = Re, V, Mo), it is found that their band structures are all rather complex and the B d states are predominant near the E_F. In the same series, the overall electronic structures are similar. The B—B bond is the strongest among the bonds with short atomic distances and stronger for compounds with A = Hf than A = Zr. The change of bond length influences the bond strength little. The variation of T_c in the same series can be explained by the strength of the B—B bonds, i.e. the stronger the bonding, the lower the T_c and so is related to the electronic effects of atom A.

REFERENCES

1. Cai Shu-Hui, Li Jun and Liu Chun-Wan, *Chin. J. Chem.* 1994, **12**, 385.
2. Cai Shu-Hui and Liu Chun-Wan, *J. Chem. Soc., Faraday Trans.* 1995, in press.
3. K. Kinoshita, *Phase Trans.* 1990, **23**, 73.
4. (a) D. D. Koelling, D. L. Johnson, S. Kirkpatrick and F. M. Mueller, *Solid State Commun.* 1971, **9**, 2039; (b) D. L. Johnson, *Phys. Rev. B* 1974, **9**, 2273.
5. T. Jarlborg and A. J. Freeman, *Phys. Rev. B* 1980, **22**, 2332.
6. R. Asokamani, G. Subramoniam, S. M. Jaya and S. Pauline, *Phys. Rev. B* 1991, **44**, 2283.

7. S. Pauline, R. Asokamani, G. Subramoniam and S. M. Jaya, *Solid State Commun.* 1992, **83**, 235.
8. S. Sankaralingam, S. M. Jaya and R. Asokamani, *J. Low Temp. Phys.* 1992, **88**, 1.
9. P. Lerch, E. G. Moroni and T. Jarlborg, *Solid State Commun.* 1993, **88**, 167.
10. F. M. Chu, M. Sob, R. Siegl, T. E. Mitchell, D. P. Pope and S. P. Chen, *Phil. Mag. B* 1994, **70**, 881.
11. R. A. deGroot, D. D. Koelling and F. M. Mueller, *J. Phys. F.* 1980, **10**, L235.
12. B. M. Klein, W. E. Pickett, D. A. Papaconstantopoulos and L. L. Boyer, *Phys. Rev. B* 1983, **27**, 6721.
13. M.-C. Huang, H. J. F. Jansen and A. J. Freeman, *Phys. Rev. B* 1988, **37**, 3489.
14. (a) S. Ishida, S. Asano and J. Ishida, *J. Phys. Soc. Jpn* 1985, **54**, 3925; (b) S. Ishida and S. Asano, *J. Phys. Soc. Jpn* 1985, **54**, 4688; (c) S. Ishida, S. Asano and J. Ishida, *J. Phys. Soc. Jpn* 1985, **54**, 4695.
15. R. L. Johnston and R. Hoffmann, *Z. Anorg. Allg. Chem.* 1992, **616**, 105.
16. R. Nesper, *Angew. Chem., Int. Edn Engl.* 1991, **30**, 789.
17. Xu Jia, Xu Guang-Xian and Wang Xiang-Yu, *Huaxue Tongxun* 1986, **3**, 46.
18. J.-Y. Saillard and R. Hoffmann, *J. Am. Chem. Soc.* 1984, **106**, 2006.
19. T. Hughbanks and R. Hoffmann, *J. Am. Chem. Soc.* 1983, **105**, 1150.
20. E. Canadell, Y. Mathey and M.-H. Whangbo, *J. Am. Chem. Soc.* 1988, **110**, 104.
21. H. Basch and H. B. Gray, *Theor. Chim. Acta* 1966, **4**, 367.
22. A. Dedieu, T. A. Albright and R. Hoffmann, *J. Am. Chem. Soc.* 1979, **101**, 3141.
23. B. T. Matthias, T. H. Geballe and V. B. Compton, *Rev. Mod. Phys.* 1963, **35**, 1.
24. V. B. Compton and B. T. Matthias, *Acta Cryst.* 1959, **12**, 651.
25. R. P. Elliott and W. Rostoker, *Trans. Am. Soc. Met.* 1958, **50**, 617.
26. R. P. Elliott, *Trans. Am. Soc. Met.* 1961, **53**, 321.
27. J. Bardeen, L. N. Cooper and J. R. Schrieffer, *Phys. Rev.* 1957, **108**, 1175.
28. W. L. McMillan, *Phys. Rev.* 1968, **167**, 331.
29. H. Stern, *Phys. Rev B.* 1975, **12**, 951.
30. A. V. Narlikar and S. N. Ekbote, *Superconductivity and Superconducting Materials*, p. 183. South Asian Publisher, New Delhi, Madras (1983).